Alexandria Engineering Journal (2020) xxx, xxx–xxx

HOSTED BY

ELSEVIER

Alexandria University

Alexandria Engineering Journal

www.elsevier.com/locate/aej
www.sciencedirect.com

Classical and fractional analysis of the effects of Silicosis in a Mining Community

H.M. Tenkam [a,*], E.F. Doungmo Goufo [b], B. Tsanou [c], A.S. Hassan [d], N. Hussaini [d], Y.A. Terefe [e]

[a] *Department of Mathematics and Applied Mathematics, North-West University, Private Bag X1290, Potchefstroom 2520, South Africa*
[b] *Department of Mathematical Sciences University of South Africa, Florida 0003, South Africa*
[c] *Department of Mathematics and Computer Science, University of Dschang, P.O. Box 67, Dschang, Cameroon*
[d] *Department of Mathematical Sciences, Bayero University, Kano, P. M. B. 3011, Nigeria*
[e] *Department of Mathematics and Applied Mathematics, University of Limpopo, Sovenga 0727, South Africa*

Received 17 December 2019; revised 28 April 2020; accepted 30 April 2020

KEYWORDS

Silicosis;
Silica dust;
Global stability

Abstract A mathematical model for the transmission dynamics of silicosis in a mining environment is designed and its qualitative analysis is given. The model takes into account the severity of silica dust exposure in a mining environment. The whole analysis is done in both fractional differentiation and classical integer calculus. In the former case, the Haar wavelet numerical scheme is used to solve the model and perform graphical representations. In the integer calculus case, it is shown that the disease free and endemic equilibria are globally asymptotically stable in the absence as well as in the presence of silica dust particles in the air, respectively. The epidemiological implications of these results are discussed. Numerical simulations are presented to support the theoretical analysis. In fractional differentiation, we show graphically via the Haar wavelet scheme the convergence to the disease free-equilibrium and the global stability of the endemic equilibrium, results successfully confirmed analytically via the classical integer analysis.

1. Introduction

The immense industrial boom of the 19th century has triggered a massive exploitation in the mining sector, resulting in serious environmental pollution and occupational health problems. The fact is that some mining companies consistently failed to employ proper measures to protect workers against excessive dust inhalation and the concomitant risks of silicosis, cancer and tuberculosis [14]. For instance, towards the end of the 1990's only 8 of 48 South African gold mines had estimated crystalline silica concentrations below the widely used reference limit of 0.1 mg/m^3 [14]. Workers are exposed to silica dust in sectors such as mining and related milling operations, construction, agricultural and ceramic industries. Furthermore,

* Corresponding author.
E-mail address: michel.djouosseutenkam@nwu.ac.za (H.M. Tenkam).
Peer review under responsibility of Faculty of Engineering, Alexandria University.

https://doi.org/10.1016/j.aej.2020.04.044

jewellery making also produces silica dust due to cutting, grinding and polishing [20,22].

Silicosis is a lung disease caused by inhalation and deposition of silica particles, resulting in a pulmonary response which can progress to tuberculosis or lung cancer [31,29]. It is characterized by a progressive deterioration of the metabolism of pulmonary macrophage, which leads to the death of cells and tissues. Symptoms of silicosis include exertional dyspnea or difficulty in breathing (shortness of breath), cough (often persistent and sometimes severe), fatigue, fever, chest pain, loss of appetite, night sweats and weight loss (Anorexia) [27]. Silicosis has no cure and prevention is the best way to avoid the disease [6,7]. Most of silicosis-related deaths seem to occur in areas associated with mining industries [23]. Furthermore, between 1968 and 2002, silicosis contributed to the death of approximately 74 million people in the U.S. [32]. There are three levels of silicosis depending on the degree and duration of cumulative exposure to the crystalline silica particles. The acute form occurs generally within a few weeks to 2 years of substantial exposure to a high concentration of silica dust, the accelerated form is caused by a medium exposure between 2 to 10 years and the symptoms of the chronic form appear more than 10 years after the first exposure to low concentration of silica dust [22]. An evaluation study on mine workers has shown that the incidence of pulmonary tuberculosis for those suffering from silicosis was 3 to 39 times higher than for those without silicosis [22]. The incidence rate was proportional to the severity of the silicosis or the level of exposure to silica dust [22,27,21,10].

In another side, differential models with derivative of fractional order and their applications have been intensively analysed in many works [1–3,15,19,24]. Even though a certain number of analyzes have been performed in the context of modeling the spread of epidemic diseases, the large majority of them were limited to models with integer order derivative. In last decades, it has been proved that number of nature phenomena portrayed by different fields in sciences, engineering and technology can be successfully and accurately described by the systems using concepts of fractional calculus. For instance, in some works, a method like Adomian decomposition has been exploited to obtain solutions of a system of nonlinear fractional differential equations. Similar technique was extended in [1], where the classical Darcy law was generalized using a complementary decomposition method, namely Frobenius method. In the paper [15], fractional calculus in epidemiology has been applied to describe the dynamics related to the outbreak of dengue fever. We are going to perform similar investigation in this paper with the application of fractional operators to a model symbolizing the transmission dynamics of silicosis in a mining environment. A comparison with the standard method will also be provided. However, we can add that from a mathematical modelling point of view, not enough has been done to understand the dynamics of the disease although some mathematical models have been described to study the risk of airborne infectious diseases, which do not capture the features of a disease like silicosis due to exhaled and inhaled air [8,12]. To the authors' best knowledge, the proposed mathematical model is the first model to study the transmission dynamics of silicosis in a mining environment. It is instructive to use a mathematical model to gain some insights into the transmission dynamics and impact of silicosis in a community, especially in a resource-poor setting, where there is no precautionary or prevention measures are taken to avoid or minimise silica dust inhalation.

The rest of the paper is organized as follows. In Section 2, the model formulation is given. The qualitative analysis of the model is provided in Section 3. Numerical simulations to support the theoretical analysis of the model are presented in Section 4, which is followed by concluding remarks in Section 5.

2. Model formulation

To formulate the silicosis mathematical model, we make the following assumptions. The total population (mining community) at time t is denoted by $H(t)$. It consists of five mutually-exclusive compartments or classes: susceptible $S(t)$, highly exposed $E_1(t)$, medium exposed $E_2(t)$, low exposed $E_3(t)$ individuals to silica dust and infected individuals with clinical symptoms of silicosis $I(t)$, so that

$$H(t) = S(t) + E_1(t) + E_2(t) + E_3(t) + I(t).$$

The flow diagram of the dynamics of the silicosis in the mining community is illustrated in Fig. 1.

We assume further that silica is found throughout the earth's crust in almost every mineral deposit and it is harmless until disturbed in a way that creates dust. The dynamics of silica dust (which is the infecting agent) at time t, denoted by $C(t)$, is mathematically given by

$$\dot{C} = M - aC - S\lambda\sum_{i=1}^{3}\gamma_i(C), \tag{2.1}$$

where $M \geqslant 0$ is the constant production of silica dust in the air-shed generated by the mining activities in the area, a is the rate at which the silica dust is lost during mining, λ is a conversion coefficient and the term

$$\gamma_i(C) = \beta_i \frac{p}{V} C = \beta_i q C, \tag{2.2}$$

for $i = 1, 2, 3$, represents the force of infection for silica dust inhalation, in which β_1, β_2 and β_3 are the effective contact rates of susceptible individuals with high, medium and low silica exposed classes, respectively. The parameter q in (2.2) is the probability of the inhaled silica not cleared by mucous or coughing. Here, $\dot{C}$ denotes the rate of change of silica dust concentration in the mining environment. In the absence of any mining activities, we assume that there is no silica in the air and M will be zero. This helps us to get a silica free environment (no silicosis).

The susceptible population, $(S(t))$, is increased by the recruitment of people into the mining community at a rate Λ. The population is decreased by infection with silicosis at a rate γ_i and natural death rate μ, which is assumed to be occur in all human compartments. Hence, the rate of change of the susceptible individuals is given by

$$\dot{S} = \Lambda - S\sum_{i=1}^{3}\gamma_i(C) - \mu S.$$

The exposed compartments, $(E_i(t))$, are generated by the infection of susceptible individuals with silicosis at the rate γ_i, and are reduced by natural death rate μ and progression to the infected compartment at the rate $\alpha_i, i = 1, 2, 3$. It is assumed that $\alpha_1^{-1} \leq 5$ years, 5 years $\leqslant \alpha_2^{-1} \leq 10$ years and $\alpha_3^{-1} \geqslant 10$ years, so that

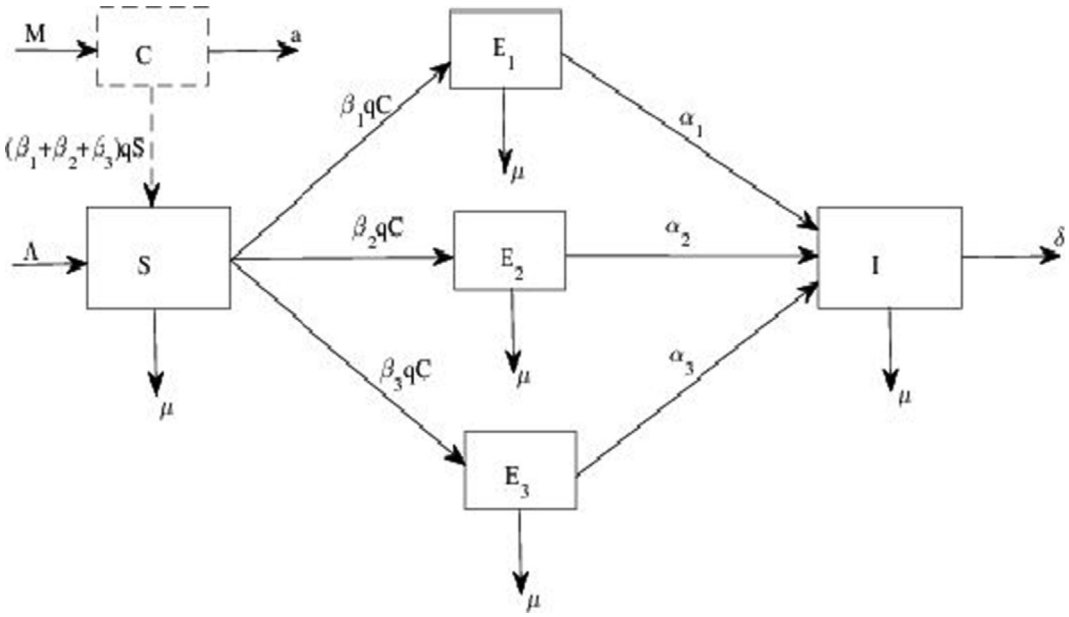

Fig. 1 Flow diagram of the model.

$$\dot{E}_i = S\gamma_i(C) - (\alpha_i + \mu)E_i \quad i = 1, 2, 3.$$

Similarly, the compartment of silicosis infected individuals $(I(t))$ is increased by the progression of silicosis exposed individuals at rates α_i and is decreased by natural and silicosis induced death rates μ and δ, respectively. Thus,

$$\dot{I} = \sum_{i=1}^{3} \alpha_i E_i - (\delta + \mu)I.$$

Putting the above equations together, the model equations for the transmission dynamics of silicosis in a mining community is given by the following system of non-linear differential equations:

$$\begin{aligned} \dot{S} &= \Lambda - S\sum_{i=1}^{3}\gamma_i(C) - \mu S, \\ \dot{E}_i &= S\gamma_i(C) - (\alpha_i + \mu)E_i \quad i = 1, 2, 3, \\ \dot{I} &= \sum_{i=1}^{3}\alpha_i E_i - (\delta + \mu)I, \\ \dot{C} &= M - aC - S\lambda\sum_{i=1}^{3}\gamma_i(C). \end{aligned} \tag{2.3}$$

By using (2.2), the system (2.3) reads as

$$\begin{aligned} &\dot{S} = \Lambda - \beta qCS - \mu S, \\ &\dot{E}_i = \beta_i qCS - \left((\alpha_i + \mu)E_i i = 1, 2, 3, \dot{I} = \sum_{i=1}^{3}\alpha_i E_i - (\delta + \mu)I, \dot{C} = M - aC - \lambda\beta qCS, \end{aligned} \tag{2.4}$$

where $\beta = \sum_{i=1}^{3}\beta_i$. Since we are dealing with human populations and silica dust concentration, all the variables and parameters are non-negative. The description of the parameters and their values are presented in Table 1.

The system (2.4) is appended with the following non negative initial conditions:

Table 1 Variables and parameters with units for the *SEI* model (2.4).

Symbols	Descriptions	Units
λ	Conversion coefficient	0.51
β_i	Effective contact rate between susceptible and silica dust	0.5, 0.35, 0.22
α_i	Progression rate (exposed to infective)	$0.12, 0.15, 0.3/\text{indiv} \cdot \text{year}$
μ	Natural death rate of individuals	$0.117\ \text{year}^{-1}$
γ_i	Forces of infection due to silica dust inhalation	year^{-1}
M	Constant dust produced	$\text{mg} \cdot \text{m}^{-3}$
δ	Disease induced death rate of individuals	$0.39\ \text{year}^{-1}$
Λ	Recruitment of susceptible individuals	20/indiv.year
C	Silica dust concentration	$\text{mg} \cdot \text{m}^{-3}$
q	Probability of the inhaled silica not cleared by coughing	0.65
a	Silica dust deposition rate	0.7

$$\begin{aligned} &S(t_0) = S^0,\ E_i(t_0) = E_i^0,\ I(t_0) = I^0, \\ &C(t_0) = C^0, \quad \text{for} \quad t_0 \geqslant 0 \quad \text{and} \quad i = 1, 2, 3. \end{aligned} \tag{2.5}$$

3. Generalized dynamics of silicosis in a mining: Fractional approach

In order broaden the view on the effects of Silicosis, we generalize the model (2.4) by applying the Caputo fractional derivative which is defined as follows [4,11,18,17,25,28]:

3.1. The Caputo fractional derivative

Let $-\infty \leqslant a < t,\ \ b > a$ and the real function $\mathbf{v} : (a,b) \longrightarrow \mathbb{R}$ be a locally integrable function. The Caputo fractional derivative in its classical version is defined for the order v, a time $t > 0$, as

$$ {}^{C}D_{t}^{v}\mathbf{v}(t) = I^{1-v}\frac{d}{dt}\mathbf{v}(t), \quad 0 < v \leqslant 1. \tag{3.1}$$

Using this derivative to solve differential equations necessitates the definition of its antiderivative. Then, the fractional integral of order v associated to the Caputo fractional derivative is given by

$$ I^{v}\mathbf{v}(t) = \frac{1}{\Gamma(v)}\int_{a}^{t}\mathbf{v}(\tau)(t-\tau)^{v-1}d\tau. \tag{3.2}$$

This leads to the generalized system modelling the dynamics of silicosis in a mining and reading as

$$\begin{aligned} {}^{C}D_{t}^{v}S &= \Lambda - \beta v CS - \mu S, \\ {}^{C}D_{t}^{v}E_{i} &= \beta_{i} v CS - ((\alpha_{i}+\mu)E_{i}\ i = 1,2,3, \\ {}^{C}D_{t}^{v}I &= \sum_{i=1}^{3}\alpha_{i}E_{i} - (\delta+\mu)I, \\ {}^{C}D_{t}^{v}C &= M - aC - \lambda\beta v CS. \end{aligned} \tag{3.3}$$

We assume that for this model, the following initial conditions hold:

$$\begin{aligned} &S(t_0) = S^0,\ E_i(t_0) = E_i^0,\ I(t_0) = I^0, \\ &C(t_0) = C^0, \quad \text{for} \quad t_0 \geqslant 0 \quad \text{and} \quad i = 1,2,3. \end{aligned} \tag{3.4}$$

To continue the analysis, a numerical approach, namely Haar wavelet numerical scheme is going to be used to address the solvability of the system (5.1)–(3.4). In the next section, the major concepts of the Haar wavelet technique are recalled.

4. Haar wavelets numerical scheme

In the literature [5,13,16,26], the Haar wavelet is defined to be the following function

$$ \mathfrak{F}(t) = \begin{cases} 1, & \text{if} \quad t \in (0,\ 1/2); \\ -1, & \text{if} \quad t \in (1/2,\ 1); \\ 0, & \text{elsewhere.} \end{cases} \tag{4.1}$$

The function is obviously defined $(-\infty, +\infty)$. Note that every $a \in \{0,1,2,3,\cdots\}$ can explicitly be expressed as $a = 2^{r} + e$ with $r = 0,1,2,\cdots$ and $e = 0,1,2,\cdots,2^{r}-1$. Taking $t \in [0,1)$ and for every $a \in \{0,1,2,3,\cdots\}$ the following family can be defined:

$$ f_{a}(t) = \begin{cases} 2^{\frac{r}{2}}\mathfrak{F}(2^{r}t - e), & \text{for} \quad a = 1,2,\cdots; \\ 1, & \text{for} \quad a = 0. \end{cases} \tag{4.2}$$

This means that $\{f_{a}(t)\}_{a=0}^{\infty}$ defines a complete orthonormal system in the space $L^{2}[0,1)$. Similarly for the function $u \in C[0,1)$, the series $\sum_{a=0}^{\infty}\langle u, f_{a}\rangle f_{a}$ is uniformly convergent to another function u where $\langle u, f_{a}\rangle = \int_{0}^{\infty}u(t)f_{a}(t)dt$. Consequently the function u take the form:

$$ u(t) = \sum_{a=0}^{\infty}\beta_{i}f_{a}(t)$$

with $\beta_{a} = \langle u, f_{a}\rangle$. Alternatively, the approximated solution can take the form

$$ u(t) \approx u_{e}(t) = \sum_{a=0}^{e-1}\beta_{i}f_{a}(t)$$

where $e \in \{2^{r} : \ \ r = 0,1,2,\cdots\}$.

Now, let $k \in \mathbb{N}$, we define the function

$$ f_{j,a}(t) = f_{a}(t - j + 1) \quad j = 1,2,\cdots,k \quad \text{and} \quad a = 0,1,2,\cdots \tag{4.3}$$

as the translation of the Haar function on $[0,k)$, with f_{a} defined by (4.2). Note that f_{a} and $f_{j,a}$ satisfy the same topological properties. Then, the family $\{f_{j,a}(t)\}_{a=0}^{\infty}, \quad (j = 1,2,\cdots,k)$ also defines a complete orthonormal system in $L^{2}[0,1)$, the space of square-integrable functions.

Moreover, we define the haar orthonormal basis functions

$$ \beta_{j,a} = \langle u, f_{j,a}\rangle = \int_{0}^{\infty}u(t)f_{j,a}(t)dt$$

which are used to expand the solution $u \in L^{2}[0,k)$ into the series

$$ u(t) = \sum_{j=1}^{k}\sum_{a=0}^{\infty}\beta_{j,a}f_{j,a}(t). \tag{4.4}$$

Practically, the solution is approximated as follows

$$ u(t) \approx u_{e}(t) = \sum_{j=1}^{k}\sum_{a=0}^{e-1}\beta_{j,a}f_{j,a}(t) \tag{4.5}$$

where $e \in \{2^{r} : \ \ r = 0,1,2,\cdots\}$. Lastly, note that (4.5) can take the compact form

$$ u(t) \approx u_{e}(t) = {}^{T}G_{ke\times 1}\mathfrak{F}_{ke\times 1}. \tag{4.6}$$

Here ${}^{T}G_{ke\times 1}$ represents the transpose vector of

$$ G_{ke\times 1} = \begin{pmatrix} \beta_{1,0} \\ \vdots \\ \beta_{1,e-1} \\ \beta_{2,0} \\ \vdots \\ \beta_{2,e-1} \\ \vdots \\ \beta_{k,0} \\ \vdots \\ \beta_{k,e-1} \end{pmatrix} \quad \text{and} \quad \mathfrak{F}_{ke\times 1} = \begin{pmatrix} f_{1,0} \\ \vdots \\ f_{1,e-1} \\ f_{2,0} \\ \vdots \\ f_{2,e-1} \\ \vdots \\ f_{k,0} \\ \vdots \\ f_{k,e-1} \end{pmatrix}.$$

5. Mathematical solvability for the generalized dynamics of silicosis in a mining

In this section, we solved numerically the generalized system of dynamics of silicosis in a mining via the Haart wavelets method. Recall that the model in its generalized form reads as

$$
\begin{aligned}
&{}^{C}D_t^{v}S = \Lambda - \beta v C S - \mu S,\\
&{}^{C}D_t^{v}E_i = \beta_i v C S - ((\alpha_i+\mu)E_i \ i=1,2,3,\\
&{}^{C}D_t^{v}I = \sum_{i=1}^{3}\alpha_i E_i - (\delta+\mu)I,\\
&{}^{C}D_t^{v}C = M - aC - \lambda\beta v C S.
\end{aligned}
\tag{5.1}
$$

We assume that for this model, the following initial conditions hold:

$$
\begin{aligned}
&S(t_0) = S^0,\ E_i(t_0) = E_i^0,\ I(t_0) = I^0,\\
&C(t_0) = C^0, \quad \text{for} \quad t_0 \geqslant 0 \quad \text{and} \quad i = 1,2,3.
\end{aligned}
\tag{5.2}
$$

To use the numerical scheme described above [19,24], let us put the system (5.1) and (5.2) into the compact form. Hence we define the vectors

$$
u(t) = \begin{pmatrix} S(t)\\ E_i(t)\\ I(t)\\ C(t)\end{pmatrix} \quad \text{and}
$$

$$
g_0(S,E_i,I,C) = u(t_0) = \begin{pmatrix} S(t_0)\\ E_i(t_0)\\ I(t_0)\\ C(t_0)\end{pmatrix} = \begin{pmatrix} \widehat{S}\\ \hat{E}_i\\ \widehat{I}\\ \widehat{C}\end{pmatrix}
$$

and we also define the matrix

$$
\begin{aligned}
\mathbf{M}(u(t),t) = &\mathbf{M}(S(t),E_i(t),I(t),C(t),t) = \begin{pmatrix} \mathbf{M}_1(u(t),t)\\ \mathbf{M}_2(u(t),t)\\ \mathbf{M}_3(u(t),t)\\ \mathbf{M}_4(u(t),t)\end{pmatrix}\\
&= \begin{pmatrix} \mathbf{M}_1(S(t),E_i(t),I(t),C(t),t)\\ \mathbf{M}_2(S(t),E_i(t),I(t),C(t),t)\\ \mathbf{M}_3(S(t),E_i(t),I(t),C(t),t)\\ \mathbf{M}_4(S(t),E_i(t),I(t),C(t),t)\end{pmatrix}
\end{aligned}
$$

where

$$
\begin{cases}
\mathbf{M}_1(u(t),t) = \Lambda - \beta v C(t) S(t) - \mu S(t),\\
\mathbf{M}_2(u(t),t) = \beta_i v C(t) S(t) - ((\alpha_i+\mu)E_i(t) \ i=1,2,3,\\
\mathbf{M}_3(u(t),t) = \sum_{i=1}^{3}\alpha_i E_i(t) - (\delta+\mu)I(t),\\
\mathbf{M}_4(u(t),t) = M - aC(t) - \lambda\beta v C(t) S(t)
\end{cases}
$$

Hence, (5.1) becomes

$$
D_t^{v}h(t) = \mathbf{M}(u(t),t)
$$

equivalent to,

$$
\begin{aligned}
&D_t^{v}S(t) = \mathbf{M}_1(u(t),t)\\
&D_t^{v}E_i(t) = \mathbf{M}_2(u(t),t)\\
&D_t^{v}I(t) = \mathbf{M}_3(u(t),t)\\
&D_t^{v}C(t) = \mathbf{M}_4(u(t),t),
\end{aligned}
\tag{5.3}
$$

still with assumption that the following initial conditions hold:

$$
\begin{aligned}
&S(0) = \widehat{S}(S),\ E_i(0) = \hat{E}_i(E_i),\ i=1,2,3.,\ I(0) = \widehat{I}(I),\\
&C(0) = \widehat{C}(C).
\end{aligned}
$$

Using the iteration in the compact form (4.6), the Haar wavelets scheme is used to approximate the silicosis model (5.3). Hence, we obtain

$$
\begin{aligned}
&D_t^{v}S(t) = \mathbf{M}_1(u(t),t) \approx D_t^{v}S_e(t) = {}^{T}G_{ke\times 1}^{1}\mathfrak{F}_{ke\times 1}\\
&D_t^{v}E_i(t) = \mathbf{M}_2(u(t),t) \approx D_t^{v}\left(E_{ie}(t) = {}^{T}G_{ke\times 1}^{2}\mathfrak{F}_{ke\times 1}, \quad i=1,2,3,\right.\\
&D_t^{v}I(t) = \mathbf{M}_3(u(t),t) \approx D_t^{v}I_e(t) = {}^{T}G_{ke\times 1}^{3}\mathfrak{F}_{ke\times 1}\\
&D_t^{v}C(t) = \mathbf{M}_4(u(t),t) \approx D_t^{v}C_e(t) = {}^{T}G_{ke\times 1}^{4}\mathfrak{F}_{ke\times 1}
\end{aligned}
\tag{5.4}
$$

The application of (3.2) on both sides of system (5.4) gives

$$
\begin{aligned}
&S(t) - \widehat{S} \approx D_t^{v}S_e(t) = {}^{T}G_{ke\times 1}^{1}B_{ke\times ke}^{v}\mathfrak{F}_{ke\times 1}\\
&E_i(t) - \hat{E}_i \approx D_t^{v}E_{ie}(t) = {}^{T}G_{ke\times 1}^{2}B_{ke\times ke}^{v}\mathfrak{F}_{ke\times 1}, \quad i=1,2,3,\\
&I(t) - \widehat{I} \approx D_t^{v}I_e(t) = {}^{T}G_{ke\times 1}^{3}B_{ke\times ke}^{v}\mathfrak{F}_{ke\times 1}\\
&C(t) - \widehat{C} \approx D_t^{v}C_e(t) = {}^{T}G_{ke\times 1}^{4}B_{ke\times ke}^{v}\mathfrak{F}_{ke\times 1}
\end{aligned}
\tag{5.5}
$$

equivalent to

$$
\begin{aligned}
&S(t) \approx S_e(t) = {}^{T}G_{ke\times 1}^{1}B_{ke\times ke}^{v}\mathfrak{F}_{ke\times 1} + \widehat{S}\\
&E_i(t) \approx E_{ie}(t) = {}^{T}G_{ke\times 1}^{2}B_{ke\times ke}^{v}\mathfrak{F}_{ke\times 1} + \hat{E}_i, \quad i=1,2,3,\\
&I(t) \approx I_e(t) = {}^{T}G_{ke\times 1}^{3}B_{ke\times ke}^{v}\mathfrak{F}_{ke\times 1} + \widehat{I}\\
&C(t) \approx C_e(t) = {}^{T}G_{ke\times 1}^{4}B_{ke\times ke}^{v}\mathfrak{F}_{ke\times 1} + \widehat{C}.
\end{aligned}
\tag{5.6}
$$

Here $B_{ke\times ke}^{v}$ is called the haar wavelets matrix of fractional order [5,13]. The use of Galerkin numerical scheme of the collocation points to solve the model (5.1) and (5.2), leads to the substitution of (5.4) and (5.6) into (5.1). We therefore obtain the residual errors caused by such a technique and reading as

$$
\begin{aligned}
&\Theta_1\varpi^1,\varpi^2,\varpi^3,\varpi^4,t\\
&= {}^{T}G_{ke\times 1}^{1}\mathfrak{F}_{ke\times 1} - \mathbf{M}_1\left({}^{T}G_{ke\times 1}^{1}B_{ke\times ke}^{v}\mathfrak{F}_{ke\times 1}, {}^{T}G_{ke\times 1}^{2}B_{ke\times ke}^{v}\mathfrak{F}_{ke\times 1}, {}^{T}G_{ke\times 1}^{3}B_{ke\times ke}^{v}\mathfrak{F}_{ke\times 1}, t\right)\\
&\Theta_2\varpi^1,\varpi^2,\varpi^3,\varpi^4,t\\
&= {}^{T}G_{ke\times 1}^{2}\mathfrak{F}_{ke\times 1} - \mathbf{M}_2\left({}^{T}G_{ke\times 1}^{1}B_{ke\times ke}^{v}\mathfrak{F}_{ke\times 1}, {}^{T}G_{ke\times 1}^{2}B_{ke\times ke}^{v}\mathfrak{F}_{ke\times 1}, {}^{T}G_{ke\times 1}^{3}B_{ke\times ke}^{v}\mathfrak{F}_{ke\times 1}, t\right)\\
&\Theta_3\varpi^1,\varpi^2,\varpi^3,\varpi^4,t\\
&= {}^{T}G_{ke\times 1}^{3}\mathfrak{F}_{ke\times 1} - \mathbf{M}_3\left({}^{T}G_{ke\times 1}^{1}B_{ke\times ke}^{v}\mathfrak{F}_{ke\times 1}, {}^{T}G_{ke\times 1}^{2}B_{ke\times ke}^{v}\mathfrak{F}_{ke\times 1}, {}^{T}G_{ke\times 1}^{3}B_{ke\times ke}^{v}\mathfrak{F}_{ke\times 1}, t\right)\\
&\Theta_4\varpi^1,\varpi^2,\varpi^3,\varpi^4,t\\
&= {}^{T}G_{ke\times 1}^{4}\mathfrak{F}_{ke\times 1} - \mathbf{M}_4\left({}^{T}G_{ke\times 1}^{1}B_{ke\times ke}^{v}\mathfrak{F}_{ke\times 1}, {}^{T}G_{ke\times 1}^{2}B_{ke\times ke}^{v}\mathfrak{F}_{ke\times 1}, {}^{T}G_{ke\times 1}^{3}B_{ke\times ke}^{v}\mathfrak{F}_{ke\times 1}, t\right)
\end{aligned}
\tag{5.7}
$$

with

$$
\varpi^1 = \beta_{1,0}^1,\cdots,\beta_{1,e-1}^1,\cdots,\beta_{k,0}^1,\cdots,\beta_{k,e-1}^1
$$

$$
\varpi^2 = \beta_{1,0}^2,\cdots,\beta_{1,e-1}^2,\cdots,\beta_{k,0}^2,\cdots,\beta_{k,e-1}^2
$$

$$
\varpi^3 = \beta_{1,0}^3,\cdots,\beta_{1,e-1}^3,\cdots,\beta_{k,0}^3,\cdots,\beta_{k,e-1}^3
$$

$$
\varpi^4 = \beta_{1,0}^4,\cdots,\beta_{1,e-1}^4,\cdots,\beta_{k,0}^4,\cdots,\beta_{k,e-1}^4
$$

where $\beta_{\cdot,\cdot}^{a}$ are defined as the components of ${}^{T}G_{\cdot\times\cdot}^{a}$.

Now we assume that

$$
\Theta_1\left(\varpi^1,\varpi^2,\varpi^3,\varpi^4,t_{j,a}\right) = 0
$$

$$
\Theta_2\left(\varpi^1,\varpi^2,\varpi^3,\varpi^4,t_{j,a}\right) = 0
$$

$$
\Theta_3\left(\varpi^1,\varpi^2,\varpi^3,\varpi^4,t_{j,a}\right) = 0
$$

$$
\Theta_4\left(\varpi^1,\varpi^2,\varpi^3,\varpi^4,t_{j,a}\right) = 0
$$

Please cite this article in press as: H.M. Tenkam et al., Classical and fractional analysis of the effects of Silicosis in a Mining Community, Alexandria Eng. J. (2020), https://doi.org/10.1016/j.aej.2020.04.044

with

$$t_{j,a} = \frac{2a-1}{2e} + j - 1, \qquad j = 1, 2, \cdots, k; \qquad a = 1, 2, \cdots, e$$

that are a ke number of collocation points. We then have

$$\beta^1_{1,0}, \cdots, \beta^1_{1,e-1}, \cdots, \beta^1_{k,0}, \cdots, \beta^1_{k,e-1}$$
$$\beta^2_{1,0}, \cdots, \beta^2_{1,e-1}, \cdots, \beta^2_{k,0}, \cdots, \beta^2_{k,e-1}$$
$$\beta^3_{1,0}, \cdots, \beta^3_{1,e-1}, \cdots, \beta^3_{k,0}, \cdots, \beta^3_{k,e-1}.$$
$$\beta^4_{1,0}, \cdots, \beta^4_{1,e-1}, \cdots, \beta^4_{k,0}, \cdots, \beta^4_{k,e-1}.$$

which are system of $4ke$ equations with $4ke$ unknowns. We obtain these unknowns by a substitution into (5.6) that yields the approximated solution to the silicosis model and given by

$$u(t) \approx \begin{pmatrix} S_e(t) \\ E_{ie}(t) \\ I_e(t) \\ C_e(t) \end{pmatrix}$$

The convergence of this method is given by the following results [5,13,16,26]:

Proposition 5.1. *Consider* $0 \leqq \leq 1, S \in H^1[0,k), E_i \in H^1[0,k)$ $i = 1,2,3, I \in H^1[0,k)$ *and* $C \in H^1[0,k)$. *If for* $e \in \{2^r : \ r = 0,1,2,\cdots\}$, *the expression with Caputo operator* $D^v_t u_e(t)$ *approximates* $D^v_t u(t)$ *using the Haar wavelet scheme, hence the quantity*

$$\|D^v_t u(t) - D^v_t u_e(t)\|_2 \leqslant \boldsymbol{n}(\boldsymbol{n}(v))^{-1}, \tag{5.8}$$

represents the exact upper bound caused by the use of such an approximation. Here $\boldsymbol{n}(v) = \frac{2\Gamma(1-v)(1-v)}{k2^v\sqrt{\frac{\left(3-3e^{(1-v)}\right)}{2^{2v}-2}+\frac{\left(3-3e^{(2-2v)}\right)}{2^{2v}-4}}}$ *and* $\boldsymbol{n} \in \mathbb{R}^+$.

6. Numerical representations of the generalized form

Now that the error committed by using Haar wavelets scheme in our context has been successfully analyzed and shown to be insubstantial, we can provide numerical simulations using the scheme presented above and the same parameter values shown in Table 1. It appears here that the fractional model displays some expected and accurate results. In fact in Fig. 2, plotted in fractional case for the derivative order $v = 0.8$, we observed by testing different initial conditions, that the solution trajectories of the system (5.1) converge to a single point believed, as we will show here below, to be the disease-free equilibrium (or silica-free environment). Similar observation is done Fig. 2 where the solution trajectories of the system (5.1) converge to a another single point believed to be the endemic equilibrium point (found in the next section). In the next section we will fix the derivative order v at one to recover the standard classical calculus and perform some analysis on the model in order to compare the results (Fig. 3).

7. Analytical studies

In this section, we study the existence, uniqueness, boundedness and positivity of the solutions of (2.4). First, we show the local existence of solutions and then we confirm the global

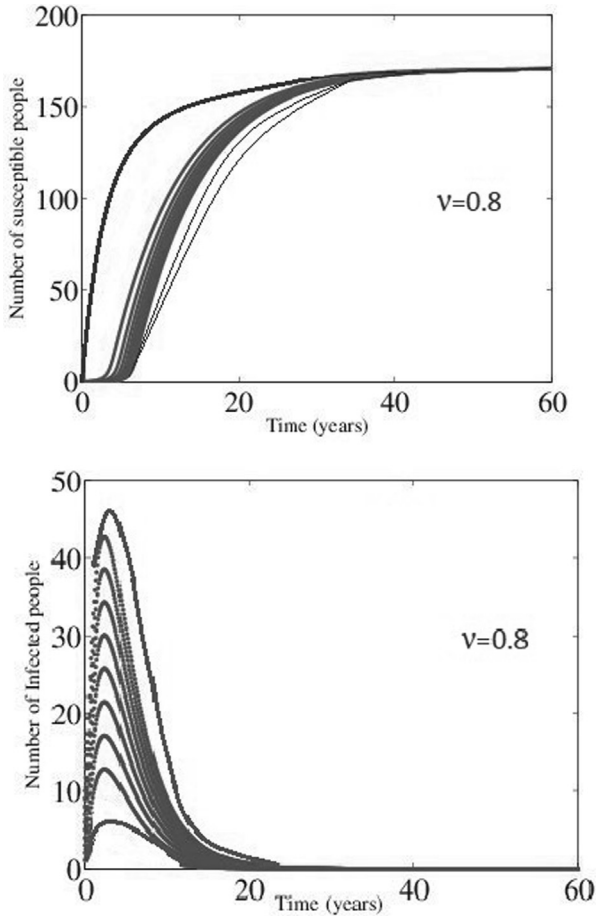

Fig. 2 Numerical simulations, for the fractional order $v = 0.8$, showing the solution trajectories of the system (5.1) converging to a single point believed, as shown in Fig. 4, to be the disease-free equilibrium (or silica-free environment). Here we take $M = 0$ and (a) $S = \frac{A}{\mu}$, (b) number of infected individuals with silicosis (0).

existence. For this purpose, we rewrite the right hand side of system (2.4) as $f(t, u(t)) = f(u(t))$, where

$$\begin{aligned} u(t) = &\ (u_1(t), u_2(t), u_3(t), u_4(t), u_5(t), u_6(t)) \\ = &\ (S(t), E_1(t), E_2(t), E_3(t), I(t), C(t)). \end{aligned}$$

Then the Cauchy problem (2.4) and (2.5) is equivalent to

$$\begin{cases} \dot{u}(t) = f(u(t)), \quad t \in [t_0, +\infty), u_i(t) \in \mathbb{R} \\ u^0_i(t_0) = u^0_i, \text{ where } u^0_i \geqslant 0. \end{cases} \tag{7.1}$$

For the existence and uniqueness of solution of (7.1), let us recall the following theorem from [9].

Theorem 7.1. *If* f *is continuous in* (t,u) *in a neighbourhood of* (t_0, u^0) *and Lipschitz continuous in* u, *then there exists a unique solution of* (7.1) *defined in a neighbourhood of* t_0. *In this study, we would like to show the existence and uniqueness of a nonnegative global solution.*

7.1. Existence of a local solution

First of all, we prove the local existence in a neighbourhood of initial time t_0.

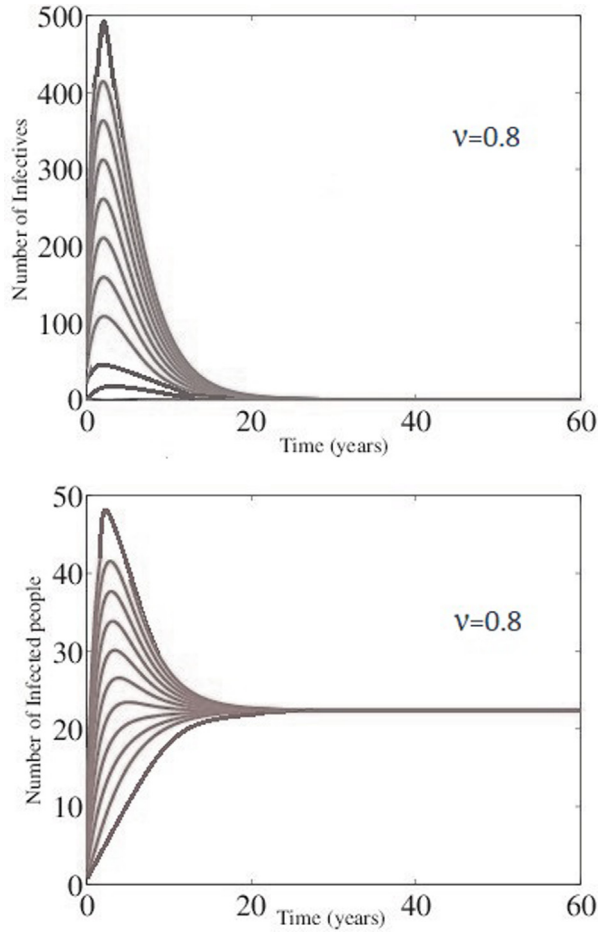

Fig. 3 Numerical simulations, for the fractional order $v = 0.8$, showing the solution trajectories of the system (5.1) converging to a single point believed, as shown in Fig. 5, to be the endemic equilibrium, and foreseing its global stability. Here we take (a) $M = 0.00001$, so that $I^* = 0.0397$, (b) $M = 90$, so that $I^* \simeq 22$.

Theorem 7.2. For the system (7.1),

(i) *there exists a local solution in neighbourhood of* t_0 *on a closed interval in* $[t_0, +\infty)$,
(ii) *the solution is non negative on its domain of definition,*
(iii) *if the solution exists, it is unique.*

Proof. (i) For any given x, let $N(x)$ denote a neighbourhood of x. Since all the parameters in Table 1 are nonnegative for all $t \in [t_0, +\infty)$, and the components of the vector fields f are readily polynomials, we infer that f is continuous on $\mathbb{R}^6$. Furthermore, since $u_i^0, i = 1, 2, \cdots 6$, are non-negative, it follows from a continuity argument that $u_i^0, i = 1, 2, \cdots 6$, are all non-negative on small neighbourhood $N(u_i^0), i = 1, 2, \cdots 6$. Define

$$N(u^0) = N(u_1^0) \times N(u_2^0) \times N(u_3^0) \times N(u_4^0) \times N(u_5^0) \times N(u_6^0).,$$

that is, $f \in \mathscr{C}(N(u^0), \mathbb{R})$. Since all spaces are finite dimensional Banach spaces, using the Cauchy-Peano theorem, there exists (not yet unique) a local solution of system (7.1) on a small enough neighbourhood (interval containing t_0) $N(t_0)$ of t_0. In case if $N(t_0)$ is not a closed interval, we can reduce it to obtain a closed one. For instance, if $N(t_0) = [t_0, t_f)$, then we choose $\overline{t_f}$ such that $t_0 < \overline{t_f} < t_f$ and $[t_0, \overline{t_f}]$ is a closed neighbourhood. We can denote it similarly by $N(t_0)$. Its compactness will be used in the proof of part (*iii*).

(ii) Now we establish the positivity of the solution on the small neighbourhood $N(t_0)$ of t_0.

Consider the first equation in (7.1) or equivalently, the first equation in (2.4):

$$\dot{u_1}(t) = \Lambda - u_1(t)\sum_{i=1}^{3}\gamma_i(u_6(t)) - \mu u_1(t),$$

$$\geqslant -\left(\sum_{i=1}^{3}\gamma_i(u_6(t)) - \mu\right)u_1(t),$$

which implies that

$$u_1(t) \geqslant u_1^0 \exp\left(\int_0^t \left[\sum_{i=1}^{3}\gamma_i(u_6(s)) - \mu\right]ds\right).$$

Therefore, $u_1(t) \geqslant 0$ at all times $t \geqslant 0$.

Similarly, from the fourth equation in (7.1), we have

$$\dot{u_6}(t) = M - au_6(t) - u_1(t)\lambda\sum_{i=1}^{3}\gamma_i(u_6(t)),$$

$$\geqslant -\left(a - u_1(t)\lambda\sum_{i=1}^{3}\gamma_i\right)u_6(t),$$

so that

$$u_6(t) \geqslant u_6^0 \exp\left(\int_0^t \left[-a - u_1(s)\lambda\sum_{i=1}^{3}\gamma_i\right]ds\right).$$

Hence, $u_6 \geqslant 0$ at all times $t \geqslant 0$.

Next, we consider the second equation in (7.1). From the positivity of u_1 and u_6, it implies that

$$\dot{u_i}(t) \geqslant -(\alpha_i + \mu)u_i(t), \quad \text{for} \quad i = 1, 2, 3,$$
$$\geqslant u_i^0 \exp(\alpha_i - \mu)t.$$

Thus u_1, u_2 and u_3 are also non-negative for all $t \geqslant 0$.

Similarly, we can prove that $u_5 \geqslant 0$ for time $t \geqslant 0$. Therefore, the local solutions of (7.1) defined on $N(t_0)$ are nonnegative as claimed in (ii).

(iii) The uniqueness of solutions follows readily from the fact that the components of the vector field f in the right hand side of (7.1) are polynomials (thus Lipschitz functions on the neighbourhood $N(t_0)$) and form the application of the Cauchy-Lipschitz theorem. □.

7.2. Existence of global solutions

Before showing that the local solutions in Theorem 7.2 are global solutions (i.e. defined on $[t_0, +\infty)$), we establish the following lemma about the boundedness of the solutions.

Lemma 7.3. *Whenever the solution of (7.1) exists, it is bounded.*

Proof. We estimate the derivative of the first unknown function $u_1(t)$ using the result of Theorem 7.2 above. Notice that

the solution is non negative on the corresponding domain (since u_1, u_2, u_3 and u_5 are positive and the remaining components are non negative). Moreover, on $N(t_0)$, we have,

$$\dot{u_1}(t) = \Lambda - \beta q u_6(t) u_1(t) - \mu u_1(t) \leqslant \Lambda - \mu u_1(t). \tag{7.2}$$

By the Gronwall inequality, from Eq. (7.2), we obtain

$$u_1(t) \leqslant \frac{\Lambda}{\mu} + \left(u_1^0 - \frac{\Lambda}{\mu}\right) e^{-\mu t},$$

and

$$\limsup_{t \to +\infty} u_1(t) \leqslant \frac{\Lambda}{\mu}.$$

Since

$$\dot{H}(t) = \Lambda - \mu H(t) - \delta u_5(t) \leqslant \Lambda - \mu H(t),$$

and

$$\dot{u_6}(t) = M - a u_6(t) - \lambda \beta q u_6(t) u_1(t) \leqslant M - a u_6(t),$$

we have similarly (after applying the Gronwall inequality twice):

$$\limsup_{t \to +\infty} H(t) \leqslant \frac{\Lambda}{\mu},$$

and

$$\limsup_{t \to +\infty} u_6(t) \leqslant \frac{M}{a}.$$

From the above bounds, if we set $H_0 = H(t_0) = u_1^0 + u_2^0 + u_3^0 + u_4^0 + u_5^0$, then the solutions of (7.1) are bounded in the following manner:

$$\begin{aligned} 0 < H(t) = & \sum_{i=1}^{5} u_i(t) \leqslant \max\left\{H_0, \tfrac{\Lambda}{\mu}\right\}; \\ 0 \leqslant u_6(t) \leqslant & \max\left\{u_6^0, \tfrac{M}{a}\right\}. \quad \square \end{aligned} \tag{7.3}$$

Remark 7.4. Due to (7.3), it is straightforward that Ω a subset of $\mathbb{R}_+^6$ satisfies

$$\begin{aligned} \Omega = & \left\{(u_1, u_2, u_3, u_4, u_5) \in \mathbb{R}_+^5 : H(t) = \sum_{i=1}^{5} u_i \leqslant \tfrac{\Lambda}{\mu}\right\} \\ & \times \left\{u_6 \in \mathbb{R}_+ : u_6(t) \leqslant \tfrac{M}{a}\right\}, \end{aligned}$$

and is positively invariant with respect to the flow of system (7.1).

By using the above results, we prove the following theorem.

Theorem 7.5. *The silicosis model (7.1) has a bounded and unique non negative solution on $[t_0, +\infty)$, where t_0 is the initial time.*

Proof. Since the solutions are bounded according to Lemma 7.3, Theorem 7.5 is a straightforward consequence of the finite time blow-up theorem of differential equations. Indeed, by setting

$$\bar{a} = \sup\left\{\dot{t}: t \text{ belongs to the defined domain of the solution}\right\},$$

we notice that $\bar{a} > t_0$. We already proved the existence of a unique solution locally in a neighbourhood $N(t_0)$. From the part where the solution exists, it stays non negative and bounded. Taking any $t^1 \in N(t_0)$ with $t^1 > t_0$, using the same argument from Theorem 7.2, we can prove that the function f is also Lipschitz in a neighbourhood $N(t^1)$ of t^1, so the solution can be extended on $N(t^1)$.

Now to prove the theorem at $\bar{a} = +\infty$, we use proof by contradiction. Hence, assume that $\bar{a} < +\infty$, and assume further that the solution can be extended to $[t_0, \bar{a})$ but not yet to $[t_0, \bar{a}]$. If $\bar{a}$ is finite then we define $u(\bar{a}) = \lim u(t)$. Due to the continuity of $\dot{u}(t)$ and the function $f(u(t))$, we have

$$\dot{u}(\bar{a}) = \lim_{t \to \bar{a}} \dot{u}(t) = \lim_{t \to \bar{a}} f(u(t)) = f(\bar{a}, u(\bar{a})).$$

Thus, the solution can be extended to $\bar{a}$. Hence, the solution exists up to $\bar{a}$ and therefore, $\bar{a}$ belongs to the defined domain of the solution of (7.1). Note that from Lemma 7.3, in finite time every component of the solution is bounded by a constant positive number. Hence, at the point $\bar{a}$, the values of function u_i are non negative and satisfy the conditions as in the proof of Theorem 7.2. Because of this, we can continue to apply Theorem 7.2 to extend the solution over a small neighbourhood $N(\bar{a})$. Denoting the radius of this neighbourhood by $\delta > 0$, the solution is also defined at $\bar{a} + \delta/2 > \bar{a}$. This contradicts with the fact that $\bar{a}$ is the supremum of all the t in the domain of the solution. Hence, we have shown that $\bar{a} = +\infty$. By virtue of Theorem 7.2, we infer that system (7.1) has a unique non negative global solution on $[t_0, +\infty)$. $\square$

7.3. Asymptotic behaviour of solutions

In this subsection, for convenience, we work with the system (2.4) rather than (7.1).

7.3.1. Simple solutions: equilibria

The equilibriums points of system (2.4) are solutions of

$$\begin{aligned} \Lambda - \beta q C S - \mu S &= 0, \\ \beta_i q C S - (\alpha_i + \mu) E_i &= 0, \quad i = 1, 2, 3 \\ \sum_{i=1}^{3} \alpha_i E_i - (\delta + \mu) I &= 0, \\ M - a C - \lambda \beta q C S &= 0. \end{aligned} \tag{7.4}$$

From the last equation of (7.4), we get

$$C = \frac{M}{(a + \lambda \beta q S)}.$$

On the other hand, from the dynamics of silicosis, if there is no silica production in the community, then it means that there are no silicosis patients in the community and clearly $M = 0$. Hence, if u_0 is the disease-free (silica-free) equilibrium point, then from (7.4), we obtain

$$u_0 = \left(\frac{\Lambda}{\mu}, 0, 0, 0, 0, 0\right). \tag{7.5}$$

Similarly, when mining workers are in state of mining production, the constant rate of silica dust production M is positive and the expected equilibrium point for system (2.4) must satisfy $M > 0$. Denoting this equilibrium by

$u^* = (S^*, E_i, I^*, C^*)$

and calling it the positive (or silicosis persistent) equilibrium point, after further simplification in (7.4), we get quadratic equation in S^*:

$$\lambda\beta q\mu(S^*)^2 + (\beta qM + \mu a - \Lambda\lambda\beta q)S^* - \Lambda a = 0, \tag{7.6}$$

and

$$\begin{aligned} E_i^* &= \frac{\beta_i q C^* S^*}{\alpha_i+\mu}, \quad i = 1,2,3 \\ I^* &= \frac{\sum_{i=1}^{3}\alpha_i E_i^*}{\mu+\delta}, \\ C^* &= M\frac{1}{a+\lambda\beta q S^*}. \end{aligned} \tag{7.7}$$

Thus, u^* is obtained by solving for the positive root S^* of (7.6) and substitute it into (7.7) to get the remaining components. We denote the discriminant of the quadratic Eq. (7.6) by

$$\Delta = (\beta qM + \mu a - \Lambda\lambda\beta q)^2 + 4\lambda\beta q\mu\Lambda a > 0,$$

and solving (7.6) gives

$$S^* = \frac{(\Lambda\lambda\beta q - \beta qM - \mu a) + \sqrt{\Delta}}{2\lambda\beta q\mu}. \tag{7.8}$$

Clearly, $S^* > 0$. Thus, the two simple solutions u_0 and u^* of (2.4) are determined. In the next subsections, we are going to show that whenever any of these equilibrium points exists, the other solutions of the system converge globally to that point.

7.3.2. Global asymptotic stability of the disease-free equilibrium

Theorem 7.6. *For $M = 0$, the unique disease-free equilibrium u_0 of (2.4) is locally asymptotically stable.*

Proof. The Jacobian matrix of (2.4) evaluated at the disease-free equilibrium u_0 is

$$J_{\mathbf{u}_0} = \begin{pmatrix} -\mu & 0 & 0 & 0 & 0 & -\beta q\frac{\Lambda}{\mu} \\ 0 & -\mu-\alpha_1 & 0 & 0 & 0 & \beta_1 q\frac{\Lambda}{\mu} \\ 0 & 0 & -\mu-\alpha_2 & 0 & 0 & \beta_2 q\frac{\Lambda}{\mu} \\ 0 & 0 & 0 & -\mu-\alpha_3 & 0 & \beta_3 q\frac{\Lambda}{\mu} \\ 0 & \alpha_1 & \alpha_2 & \alpha_3 & -\mu-\delta & 0 \\ 0 & 0 & 0 & 0 & 0 & -a-\lambda\beta q\frac{\Lambda}{\mu} \end{pmatrix}.$$

The eigenvalues of $J_{\mathbf{u}_0}$ are $-\alpha_2-\mu, -\mu, -\alpha_1-\mu, -\delta-\mu, -\mu-\alpha_3, -\frac{1}{\mu}(a\mu + q\Lambda\beta\lambda)$ and all are negative. Thus u_0 is locally asymptotically stable. □

Theorem 7.7. *For $M = 0$, the system (2.4) has a unique disease-free equilibrium u_0 which is globally asymptotically stable.*

Proof. To prove the global asymptotic stability we make use of Lyapunov-LaSalle's Principle [30] by defining the following function:

$$L_0(u) = L_0(S, E_i, I, C) = \lambda\sum_{i=1}^{3}E_i + \lambda I + C,$$

where $u = (S, E_i, I, C)$ and $L_0(u) > 0$ for $u_0 \neq u \in \Omega$. Hence, L_0 is a positive definite on Ω. The Lie derivative of L_0 , denoted by $\dot{L}_0$, in the direction of the vector field given by the right-hand side of (2.4) is

$$\dot{L}_0 = -\left[\lambda\mu\sum_{i=1}^{3}E_i + \lambda(\mu+\delta)I + aC\right] \leqslant 0.$$

Thus, $\dot{L}_0$ is a negative definite. Moreover, $\dot{L}_0 = 0$ if only if $E_i = I = C = 0, i = 1,2,3$. Hence, the largest invariant subset $\mathscr{M}_0$ contained in $\mathscr{E}_0 = \{(S, E_i, I, C) : \dot{L}_0 = 0\}$ is obtained by setting $E_i = I = C = 0$ in the equation $\dot{S} = \Lambda - \beta qCS - \mu S$ and gives $S(t) = \Lambda/\mu + [S_{(0)-\Lambda/\mu}]e^{-\mu t}$. Thus, as $t \to \infty, S(t) \to \Lambda/\mu$, and $\mathscr{M}_0 = \{u_0\}$. By LaSalle's Invariance Principle, we conclude that u_0 is globally asymptotically stable. □

7.3.3. Global asymptotic stability of the positive equilibrium

Theorem 7.8. *For $M = 0$, the unique positive equilibrium u^* of (2.4) is locally asymptotically stable.*

Proof. The Jacobian matrix of (2.4) evaluated at the positive equilibrium point u^* is

$$J_{\mathbf{u}^*} = \begin{pmatrix} -\beta qC^*-\mu & 0 & 0 & 0 & 0 & -\beta qS^* \\ \beta_1 qC^* & -\alpha_1-\mu & 0 & 0 & 0 & \beta_1 qS^* \\ \beta_2 qC^* & 0 & -\alpha_2-\mu & 0 & 0 & \beta_2 qS^* \\ \beta_3 qC^* & 0 & 0 & -\alpha_3-\mu & 0 & \beta_3 qS^* \\ 0 & \alpha_1 & \alpha_2 & \alpha_3 & -\delta-\mu & 0 \\ -\lambda\beta qC^* & 0 & 0 & 0 & 0 & -a-\lambda\beta qS^* \end{pmatrix}$$

It is easy to see that the eigenvalues of $J_{\mathbf{u}^*}$ are: $-\alpha_1-\mu < 0, -\alpha_2-\mu < 0, -\delta-\mu < 0, -\mu-\alpha_3 < 0$ and those of the following 2×2 matrix have negative real parts:

$$J_2 = \begin{pmatrix} -\beta qC^*-\mu & -\beta qS^* \\ -\lambda\beta qC^* & -a-\lambda\beta qS^*. \end{pmatrix}.$$

Because, the trace of J_2 is negative and its determinant $\mu(a+\lambda\beta qS^*) + a\beta qC^*$ is positive. Thus u^* is locally asymptotically stable. □

Theorem 7.9. *Whenever the constant production rate of silica dust M is positive, the unique positive equilibrium point u^* of system (2.4) is globally asymptotically stable.*

Proof. To establish the global asymptotic stability of u^*, since I does not appear in the remaining equations of the model, we can decouple the dynamics of I from the system and propose the following Volterra type Lyapunov functional:

$$\begin{aligned} V = &\left[S - S^* - \ln\frac{S}{S^*}\right] + \sum_{i=1}^{3}\left[E_i - E_i^* - \ln\frac{E_i}{E_i^*}\right] \\ &+ \frac{1}{\lambda}\left[C - C^* - \ln\frac{C}{C^*}\right]. \end{aligned} \tag{7.9}$$

We note that V is defined, continuous in Ω and positive definite with respect to $u = u^*$ in Ω. Furthermore, the global minimum $V = 0$ occurs at the endemic equilibrium u^*. We compute the derivative of V along the trajectories of the system (2.4)

$$\begin{aligned}\dot{V} &= (1-\tfrac{S^*}{S})\dot{S}+\sum_{i=1}^{3}\Big(1-\tfrac{E_i^*}{E_i}\Big)\dot{E}_i+(1-\tfrac{C^*}{C})\dot{C}\\ &= (1-\tfrac{S^*}{S})(\Lambda-\beta qCS-\mu S)+\sum_{i=1}^{3}\Big[\Big(1-\tfrac{E_i^*}{E_i}\Big)(\beta_i qCS-(\alpha_i+\mu)E_i)\Big]\\ &\quad+\tfrac{1}{\lambda}(1-\tfrac{C^*}{C})(M-aC-\lambda\beta qCS)\end{aligned} \tag{7.10}$$

Taking into account the endemic steady state of the model where $\Lambda=\beta qC^*S^*+\mu S^*$, $\beta_i qC^*S^*=(\alpha_i+\mu)E_i^*=0$, $M=aC^*+\lambda\beta qC^*S^*$, it follows that

$$\begin{aligned}(1-\tfrac{S^*}{S})\dot{S} &= \Lambda-\beta qCS-\mu S-\tfrac{S^*}{S}\Lambda+\beta qCS^*+\mu S^*\\ &= \Lambda(1-\tfrac{S^*}{S})-(\beta qC+\mu)(S-S^*)\\ &= (\beta qC^*S^*+\mu S^*)(1-\tfrac{S^*}{S})+S^*(\beta qC+\mu)(1-\tfrac{S}{S^*})\\ &= \mu S^*(1-\tfrac{S^*}{S})+\mu S^*(1-\tfrac{S}{S^*})+\beta qC^*S^*(1-\tfrac{S^*}{S})+\beta qCS^*(1-\tfrac{S}{S^*})\\ &= \mu S^*(2-\tfrac{S^*}{S}-\tfrac{S}{S^*})+\beta qC^*S^*(1-\tfrac{S^*}{S})+\beta qCS^*(1-\tfrac{S}{S^*})\\ &= \mu S^*(2-\tfrac{S^*}{S}-\tfrac{S}{S^*})+\sum_{i=1}^{3}\beta_i qC^*S^*(1-\tfrac{S^*}{S})+\sum_{i=1}^{3}\beta_i qCS^*(1-\tfrac{S}{S^*}),\end{aligned} \tag{7.11}$$

$$\begin{aligned}\sum_{i=1}^{3}\Big(1-\tfrac{E_i^*}{E_i}\Big)\dot{E}_i &= \sum_{i=1}^{3}(\beta_i qCS-(\alpha_i+\mu)E_i)-\sum_{i=1}^{3}\tfrac{E_i^*}{E_i}(\beta_i qCS-(\alpha_i+\mu)E_i)\\ &= \sum_{i=1}^{3}\Big(\beta_i qCS-\beta_i qC^*S^*\tfrac{E_i}{E_i^*}\Big)-\sum_{i=1}^{3}\beta_i qC^*S^*\tfrac{CSE_i^*}{C^*S^*E_i}+\sum_{i=1}^{3}\beta_i qC^*S^*,\end{aligned} \tag{7.12}$$

and

$$\begin{aligned}(1-\tfrac{C^*}{C})\dot{C} &= (aC^*+\lambda\beta qC^*S^*)(1-\tfrac{C^*}{C})-(aC+\lambda\beta qCS)(1-\tfrac{C^*}{C})\\ &= aC^*(1-\tfrac{C^*}{C})-aC(1-\tfrac{C^*}{C})+\lambda\beta qC^*S^*(1-\tfrac{C^*}{C})-\lambda\beta qCS(1-\tfrac{C^*}{C})\\ &= aC^*(2-\tfrac{C^*}{C}-\tfrac{C}{C^*})+\lambda\beta qC^*S^*(1-\tfrac{C^*}{C})-\lambda\beta qCS(1-\tfrac{C^*}{C})\end{aligned} \tag{7.13}$$

Substituting (7.11)–(7.13) into (7.10) leads to

$$\begin{aligned}\dot{V} &= \mu S^*(2-\tfrac{S^*}{S}-\tfrac{S}{S^*})+\sum_{i=1}^{3}\beta_i qC^*S^*(1-\tfrac{S^*}{S})+\sum_{i=1}^{3}\beta_i qCS^*(1-\tfrac{S}{S^*})\\ &\quad+\sum_{i=1}^{3}(\beta_i qCS-\beta_i qC^*S^*+\beta_i qC^*S^*-\beta_i qC^*S^*\tfrac{E_i}{E_i^*})+\sum_{i=1}^{3}\beta_i qC^*S^*\Big(1-\tfrac{CSE_i^*}{C^*S^*E_i}\Big)\\ &\quad+\tfrac{a}{\lambda}C^*(2-\tfrac{C^*}{C}-\tfrac{C}{C^*})+\beta qC^*S^*(1-\tfrac{C^*}{C})-\beta qCS(1-\tfrac{C^*}{C})\end{aligned}$$

or

$$\begin{aligned}\dot{V} &= \mu S^*(2-\tfrac{S^*}{S}-\tfrac{S}{S^*})+\sum_{i=1}^{3}\beta_i qC^*S^*(1-\tfrac{S^*}{S})+\sum_{i=1}^{3}\beta_i qCS^*(1-\tfrac{S}{S^*})+\sum_{i=1}^{3}\beta_i qCS(1-\tfrac{C^*S^*}{CS})\\ &\quad+\sum_{i=1}^{3}\beta_i qC^*S^*\Big(1-\tfrac{E_i}{E_i^*}\Big)+\sum_{i=1}^{3}\beta_i qC^*S^*\Big(1-\tfrac{CSE_i^*}{C^*S^*E_i}\Big)+\tfrac{a}{\lambda}C^*(2-\tfrac{C^*}{C}-\tfrac{C}{C^*})\\ &\quad+\sum_{i=1}^{3}\beta_i qC^*S^*(1-\tfrac{C^*}{C})-\sum_{i=1}^{3}\beta_i qCS(1-\tfrac{C^*}{C})\end{aligned} \tag{7.14}$$

Further rearrangements lead to

$$\begin{aligned}\dot{V} &= \mu S^*(2-\tfrac{S^*}{S}-\tfrac{S}{S^*})+(2-\tfrac{C^*}{C}-\tfrac{C}{C^*})+\sum_{i=1}^{3}\beta_i qC^*S^*\Big(4-\tfrac{S^*}{S}-\tfrac{E_i}{E_i^*}-\tfrac{C^*}{C}-\tfrac{CSE_i^*}{C^*S^*E_i}\Big)\\ &\quad+\sum_{i=1}^{3}\beta_i qCS(1-\tfrac{C^*S^*}{CS})+\sum_{i=1}^{3}\beta_i qCS^*(1-\tfrac{S}{S^*})-\sum_{i=1}^{3}\beta_i qCS(1-\tfrac{C^*}{C})\\ &= \mu S^*(2-\tfrac{S^*}{S}-\tfrac{S}{S^*})+(2-\tfrac{C^*}{C}-\tfrac{C}{C^*})+\sum_{i=1}^{3}\beta_i qC^*S^*\Big(4-\tfrac{S^*}{S}-\tfrac{E_i}{E_i^*}-\tfrac{C^*}{C}-\tfrac{CSE_i^*}{C^*S^*E_i}\Big)\\ &\quad+\sum_{i=1}^{3}\beta_i qCS[(1-\tfrac{C^*S^*}{CS})+\tfrac{S^*}{S}(1-\tfrac{S}{S^*})+\tfrac{C^*}{C}(1-\tfrac{C}{C^*})]\end{aligned} \tag{7.15}$$

$$\begin{aligned}\dot{V} &\leqslant \mu S^*(2-\tfrac{S^*}{S}-\tfrac{S}{S^*})+(2-\tfrac{C^*}{C}-\tfrac{C}{C^*})\\ &\quad+\sum_{i=1}^{3}\beta_i qC^*S^*\Big(4-\tfrac{S^*}{S}-\tfrac{E_i}{E_i^*}-\tfrac{C^*}{C}-\tfrac{CSE_i^*}{C^*S^*E_i}\Big)\\ &\quad+\sum_{i=1}^{3}\beta_i qCSm(3-\tfrac{S}{S^*}-\tfrac{C}{C^*}-\tfrac{C^*S^*}{CS}),\end{aligned} \tag{7.16}$$

where $m=\min\big(1,\tfrac{S^*}{S},\tfrac{C^*}{C}\big)$ Applying the arithmetic-geometric inequality to (7.16), we obtain $\dot{V}\leqslant 0$ for all $u\in\Omega$ and $\dot{V}=0$ if only if $u=u^*$. Hence $\mathscr{M}=\{u\in\Omega:\dot{V}=0\}=\{u^*\}$ is the largest invariant subset. From LaSalle's Invariance Principle [30], u^* is globally asymptotically stable. □

8. Numerical simulation

In this section, we present numerical simulations in order to support the theoretical results proved in the previous sections. In Fig. 4, by using different initial conditions, we observed that the solution profiles of the system (2.4) converge to the disease-free equilibrium (or silica-free environment). This result

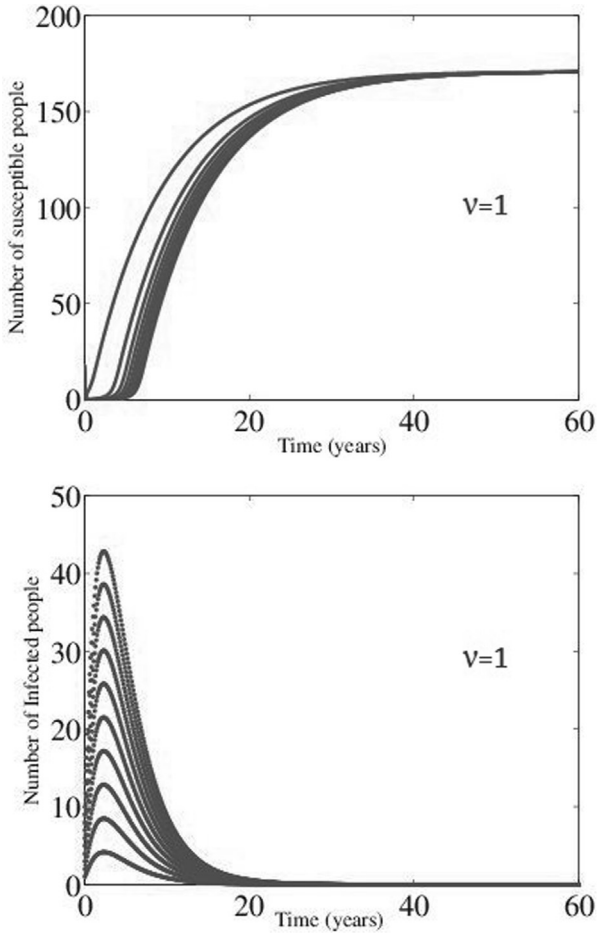

Fig. 4 Global stability of the disease-free equilibrium point when $M=0$ and (a) $S=\frac{\Lambda}{\mu}$, (b) number of infected individuals with silicosis (0).

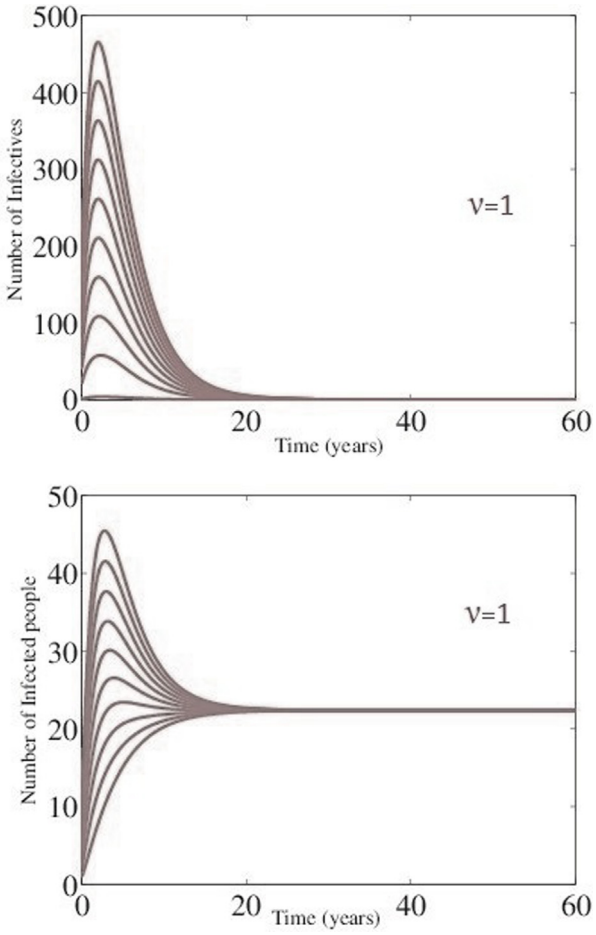

Fig. 5 Global stability of the endemic equilibrium point when (a) $M = 0.00001$, so that $I^* = 0.0397$, (b) $M = 90$, so that $I^* \simeq 22$.

implies that the disease-free equilibrium is globally asymptotically stable whenever the mining area is free from silica concentration (i.e. $M = 0$) as proved in Theorem 7.7. In the presence of silica production (i.e., $M > 0$), a unique endemic equilibrium exists and it is globally asymptotically stable (see Fig. 5). To show the effect of silica dust in the environment, we use a small value of $M = 0.00001$ in Fig. 5 (a) and it illustrate the global asymptotic stability of $I^* = 0.0397$. Using the same initial conditions with M large in Fig. 5 (b), the endemic equilibrium, is also depicted to be globally asymptotically stable, with $I^* \simeq 22$. The relation between the production of silica in the mining and the number of new silicosis infected individuals is illustrated in Fig. 6. From the same figure, we can observe that the silicosis dynamics doesn't change significantly once the environment reached into silica saturated rate. To perform all the simulations, we used the parameter values given in Table 1.

9. Conclusion

As a starting point in modelling silicosis infection, we have provided a simple ordinary differential equations model for the dynamics of the silicosis disease in a mining community is designed and subsequently analysed. The whole analysis

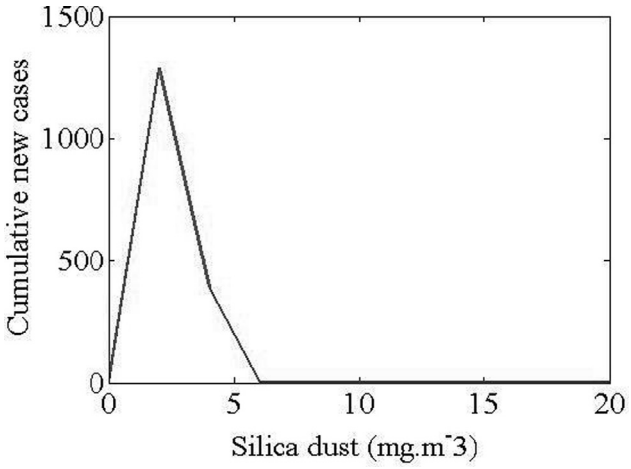

Fig. 6 The effect of silica dust on the new cases of Silicosis.

has been done in both fractional differentiation and classical integer calculus. In the former case, the Haar wavelet numerical scheme has been used to solve the model and perform graphical representations. In the classical integer calculus, it is shown that the disease-free equilibrium point exists in the absence of silica dust in the environment and is globally asymptotically stable. The biological implication of this result is that the disease doesn't invade the community irrespective of the initial size population in the community. Furthermore, it has been proven that whenever workers are exposed to crystalline silica particles, the endemic equilibrium exists and is globally asymptotically stable. Most of those results concur with those found in fractional differentiation where the global stability of the endemic equilibrium were shown graphically via the Haar wavelet scheme.

The given model is relatively simple and it captures some basic features of the silicosis exposure dynamics. However, if it enters in an environment where Tuberculosis (TB) is epidemic, co-infection will happen and the problem becomes too complicated. For such a case, we need to propose a more general model which incorporates some additional realities of the silicosis transmission dynamics. Future directions for our work include fitting the model to estimate the parameters and proposing a non-standard finite difference scheme that replicates the properties of the continuous model.

Moreover, since silicosis disease can cause Tuberculosis which is an aerosol transmitted disease, it will be very interesting to couple an advection-diffusion model (e.g. atmospheric dispersion modelling framework) for the dynamics of silica dust with a reaction model for Tuberculosis. In this new setting of partial differential equations, one could investigate the existence of travelling waves solutions. This more complicated project is under investigation by the authors as a second step on this adventure.

Declaration of Competing Interest

The authors declare that they have no known competing financial interests or personal relationships that could have appeared to influence the work reported in this paper.

Please cite this article in press as: H.M. Tenkam et al., Classical and fractional analysis of the effects of Silicosis in a Mining Community, Alexandria Eng. J. (2020), https://doi.org/10.1016/j.aej.2020.04.044

References

[1] A. Atangana, Goufo E. Doungmo, On the mathematical analysis of Ebola hemorrhagic fever: deathly infection disease in West African countries, BioMed Res. Int. (2014), https://doi.org/10.1155/2014/261383. Article ID 261383.
[2] A. Atangana, E.F. Doungmo Goufo, Computational analysis of the model describing HIV infection of CD4 + T cells, BioMed Res. Int. (2014) 7 doi: 10.1155/2014/618404. Article ID 618404.
[3] A. Atangana, A. Akgul, Can transfer function and Bode diagram be obtained from Sumudu transform, Alexandria Eng. J. (2020) (in press).
[4] A. Atangana, A. Akgul, M.O. Kolade, Analysis of fractal fractional differential equations, Alexandria Eng. J. (2020) [in press].
[5] E. Babolian, A. Shahsavaran, Numerical solution of nonlinear fredholm integral equations of the second kind using Haar wavelets, J. Comput. Appl. Math. 225 (2009) 87–95.
[6] K.M. Bang, J.M. Mazurek, Silicosis mortality, prevention, and control United States, 1968–2002, Morbidity and Mortality Weekly Report 54 (16) (2005) 401–405.
[7] K.M. Bang, J.M. Mazurek, J.M. Wood, G.E. White, S.A. Hendricks, A. Weston, Silicosis mortality trends and new exposures to respirable crystalline silica? United States, 2001–2010, Morbidity and Mortality Weekly Report 64 (2015) 117–120.
[8] S. Basu, A. Galvani, The transmission and control of XDR TB in South Africa: an operation research and mathematical modelling approach, Epidemiol. Infect. 136 (2008) 1585–1598.
[9] R.L. Burden, J.D. Faires, Numerical Analysis, Brooks/Cole Cengage Learning, 2011.
[10] G. Calvert, F. Rice, J. Boiano, J. Sheehy, W. Sanderson, Occupational silica exposure and risk of various diseases: an analysis using death certificates from 27 states of the United States, Occup. Environ. Med. 60 (2003) 122–129.
[11] M. Caputo, Linear models of dissipation whose Q is almost frequency independent–II, Geophys. J. Int. 13 (1967) 529–539, Reprinted in: Fract. Calc. Appl. Anal. 11, No 1, 3–14 (2008).
[12] M. Chacha, M. Nicola, W. Robin, Modelling the risk of airborne infectious disease using exhaled air, J. Theor. Biol. 372 (2015) 100–106.
[13] Y. Chen, M. Yi, C. Yu, Error analysis for numerical solution of fractional differential equation by Haar wavelets method, J. Comput. Sci. 3 (2012) 367–373.
[14] Department of Labour of the Republic of South Africa, National Programme for the Elimination of Silicosis. http://www.labour.gov.za/DOL/downloads/documents/useful-documents/occupational-health-and-safety/Useful%20Document%%20-%20OHS%20-%20National%20Programme%20for%20the%20Elimination%20of%20Silicosis.pdf, 10/11/2016.
[15] K. Diethelm, A fractional calculus basedmodel for the simulation of an outbreak of dengue fever, Nonlinear Dyn. 71 (4) (2013) 613–619.
[16] E.F. Doungmo Goufo, Solvability of chaotic fractional systems with 3D four-scroll attractors, Chaos, Solitons Fract. 104 (2017) 443–451, https://doi.org/10.1016/j.chaos.2017.08.038.
[17] E.F. Doungmo Goufo, Chaotic processes using the two-parameter derivative with non-singular and non-local kernel: Basic theory and applications, Chaos: Interdiscipl. J. Nonlinear Sci. 26 (2016) 084305.
[18] E.F. Doungmo Goufo, A. Atangana, Analytical and numerical schemes for a derivative with filtering property and no singular kernel with applications to diffusion, Eur. Phys. J. Plus 131 (2016) 269.
[19] E.F. Doungmo Goufo, R. Maritz, J. Munganga, Some properties of Kermack-McKendrick epidemic model with fractional derivative and nonlinear incidence, Adv. Differ. Eq. 2014 (2014) 278, https://doi.org/10.1186/1687-1847-2014-278.
[20] L. Elizabeth et al, Risk factors for pulmonary mycobacterial disease in South Africa gold miners, Am. J. Respir. Crit. Care Med. 159 (1999) 94–99.
[21] A. Farasi, M. Jabbarias, Silico-tuberculosis and associated risk factors in central province of Iran, Pan Afr. Med. J. doi:10.11604/pamj.2015.20.333.4993.
[22] C.E. Galvo Barboza, D.H. Winter, M. Seiscento, Santos U. Paula, M.T. Filho, Tuberculosis and Silicosis: epidemiology, diagnosis and chemoprophylaxis, J. Bras. Pneumol. 34 (11) (2008) 961–968.
[23] D.D. Glenn, Current issues surrounding silica, Professional Safety 53 (2) (2008) 37–46.
[24] E.F.D. Goufo, A. Atangana, Modulating chaotic oscillations in autocatalytic reaction networks using atangana–baleanu operator, Fractional Derivatives with Mittag-Leffler Kernel (Springer) 135–158 (2019).
[25] E.F.D. Goufo, M. Mbehou, M.M.K. Pene, A peculiar application of Atangana–Baleanu fractional derivative in neuroscience: Chaotic burst dynamics, Chaos, Solitons Fract. 115 (2018) 170–176.
[26] Ü. Lepik, H. Hein, Haar Wavelets: With Applications, Springer Science & Business Media, 2014.
[27] E. Hnizdo, J. Murray, Risk of pulmonary tuberculosis relative to silicosis and exposure to silica dusts in South Africa gold miners, Occup. Environ. Med. 55 (1998) 496–502.
[28] M.O. Kolade, A. Atangana, A. Akgul, Modelling and analysis of fractal-fractional partial differential equations: application to reaction-diffusion model, Alexandria Eng. J. (2020) [in press].
[29] A.K. Klein, J.P. Christopher, Evaluation of crystalline silica as a threshold carcinogen, Scand. J. Work Environ. Health. 21 (1995) 95–98.
[30] J.L. Lasalle, The Stability of Dynamical Systems, SIAM, Philadelphia, PA, 1976.
[31] M. Numinen, Mathematical modelling of risk assessment for health effect of silica exposure, Worksafe Autralia, National Institute Report, 1996.
[32] C.R. Thomas, T.R. Kelley, A Brief Review of silicosis in the United states, Environ. Health Insights 4 (2010) 21–26.